On Oxygen Plasma-Treated Polypropylene Interfaces with Air, Water, and Epoxy Resins. II. Epoxy Resins

E. OCCHIELLO,[1] M. MORRA,[1] G. MORINI,[1]* F. GARBASSI,[1†] and D. JOHNSON[2]

[1]Istituto Guido Donegani S.p.A., 4 via Fauser, 28100 Novara, Italy, and
[2]UMIST, Dept. of Chemistry, P.O. Box 88, Manchester M60 1QD, UK

SYNOPSIS

XPS, SEM, SSIMS, FTIR-ATR, water-in-air, and air-in-water contact angle measurements have been used to unambiguously characterize the locus of failure of PP/epoxy joints. In the case of untreated PP, the fracture has been found adhesive, whereas in oxygen plasma-treated PP, it is cohesive, within bulk PP, but close to the modified PP-bulk PP interface. The smoothness of fracture surfaces allowed us to exclude mechanical interlocking effects. Shear-strength measurements showed that the mechanical strength of the joint was improved by plasma treatment. Preliminary thermal equilibration of the plasma-treated PP sample and changes in the curing cycle of the epoxy resin did not change either the locus of failure or the shear strength of the joint. The reason is probably because the number of polar functions left at the surface after thermal equilibration is sufficient to induce adhesion. The mechanical strength of the PP surface layer may be the determining factor. Fracture energy calculations showed that the observed locus of failure is the same as predicted on the basis of surface energy considerations.

INTRODUCTION

Plasma treatments have been used to improve adhesion properties of polyolefin surfaces,[1-3] even if the driving force for adhesion is still very much controversial, as reviewed on several occasions.[1,4-7]

In the first part of this work, we described the effect of interfacing oxygen plasma-treated polypropylene (PP) with air and water.[8] In the present part, we study the interface of untreated and oxygen plasma-treated PP with epoxy resins, i.e., adhesion between the two materials. The main method we used was the characterization of fracture surfaces. In the previous literature, a number of examples of this approach can be found.[1,5,9-11] To profile into the sides of the fracture, we used spectroscopic methods with increasing thickness of the analyzed layer, namely, SSIMS (static secondary ion mass spectroscopy, analyzing about 1 nm), XPS (X-ray photoelectron spectroscopy, observed layer about 5 nm), and FTIR-ATR (Fourier transform infrared-attenuated total reflectance, looking at a 300–500 nm thick layer, with a germanium prism). Surface morphologies were studied by SEM and surface energies by water contact angle measurement. Mechanical strengths of PP–epoxy joints were evaluated using shear-strength methods.

The localization of fracture in adhesive joints was then found to occur as predicted by fracture energy or by adhesion calculations.[1,12,13]

EXPERIMENTAL

Oxygen plasma treatments were performed using the procedures described in Part I.[8] Plaques, 2.5 mm thick, of isotactic polypropylene (SP179 grade, Himont) were used, cut into 25 × 100 mm strips for mechanical testing. Some samples were aged in air atmosphere at 363 and 393 K to study the effect of aging on adhesion. For SSIMS studies, some samples

* Present address: Himont Italia, Centro Ricerche Novara, 4 via Fauser, 28100 Novara, Italy.
† To whom correspondence should be addressed.

Journal of Applied Polymer Science, Vol. 42, 2045–2052 (1991)
 CCC 0021-8995/91/072045-08$04.00

were treated with $^{18}O_2$ plasma. The enriched gas was provided by MSD (Merck Sharp and Dohme) with 99% isotopic purity. The plasma parameters were the same as for $^{16}O_2$ plasma.

PP–epoxy joints were prepared using a commercial epoxy adhesive (Permabond E11). Two cure cycles were performed in the E11 case, 1 h at 353 K (as suggested by the manufacturer) and 1 h at 393 K. The joint preparation and geometry were made in agreement with the ASTM D1002-72 procedure, which was also followed for shear-strength measurements. An Instron TMSM electromechanical dynamometer was used.

Water-in-air and air-in-water contact angles were obtained by the sessile drop technique on a Ramé-Hart contact angle goniometer. Advancing (aa) and receding (ra) angles were obtained by increasing or decreasing the drop volume until moving the three-phase boundary over the surface. We kept the capillary pipette of the microsyringe immersed in the drop during the entire measurement.[1] The reported values are the average over at least 10 different measurements, performed in different parts of the sample surface. The typical error is ±3 degrees.

XPS spectra were obtained using a PHI model 548 XPS spectrometer. SSIMS studies were performed using a VG quadrupole-based SIMSLAB instrument. SEM micrographs were obtained using a Cambridge Stereoscan 604 microscope. FTIR-ATR was performed using a Perkin-Elmer PE-1800 FTIR spectrometer, using a germanium internal reflection element (IRE) and a 45° incidence angle. All fracture surfaces were obtained with the same procedure used for shear strength measurements for reproducibility purposes. More details on the experimental procedures can be found in Part I of this work.[8]

RESULTS

The change in interfacial properties induced by oxygen plasma treatment was tested using a commercial thermoplastic adhesive (Permabond E11). We observed in Part I of this work[8] that aging the plasma-treated PP samples in air at high temperature for a few hours led the surface to a steady state, characterized by a water advancing angle identical to untreated PP and by a stable temperature-dependent receding angle, lower than that of PP because of the presence at the surface of a residual amount of oxygen-containing groups. This aging process will be hereinafter referred to as thermal equilibration. To find out whether the wettability of the treated surface influenced the strength of the adhesive joint and the locus of failure, we contacted the sample with the adhesive just after plasma treatment (high wettability) and after thermal equilibration in air at 363 and 393 K (low wettability).

We also studied the possible effect of different mobility of macromolecules on interfacial interactions. In this case, we changed the hardening cycle of the adhesive; in particular, we used two cure temperatures: 353 and 393 K. Of course, the latter temperature should guarantee a higher mobility of PP (modified and nonmodified) macromolecules.

Shear Strengths of Adhesive Joints

In Table I, the shear strengths we obtained are reported. The improvement after plasma treatment is clearly visible in all cases. Furthermore, the thermal equilibration of the treated surface does not seem to affect the mechanical properties of the interface. In fact, the shear strengths obtained for both the just-treated sample (aa 24°, ra 10°) and the treated sample (aa 95°, ra 40° for aging at 363 K, 50° at 393 K) are not significantly different. Also, the different mobility of macromolecular chains during hardening of the epoxy adhesive, obtained curing at 353 and 393 K, did not affect the mechanical strength of the joint.

Fracture Surfaces: Contact Angles and SSIMS

First of all we performed a morphological characterization of fracture surfaces, using SEM. In all cases, the fracture surfaces were smooth.

Table I Shear Strengths of PP/Epoxy Bonds

Sample	Shear Strength (N/mm^2)
E11 adhesive, cured 1 h at 353 K, untreated PP	0.2 ± 0.01
E11 adhesive, cured 1 h at 353 K, PP immediately after treatment	1.4 ± 0.5
E11 adhesive, cured 1 h at 353 K, PP aged 2 h 363 K	1.3 ± 0.2
E11 adhesive, cured 1 h at 393 K, PP immediately after treatment	1.0 ± 0.3
E11 adhesive, cured 1 h at 393 K, PP aged 2 h 393 K	0.9 ± 0.1

With the aim of identifying the locus of failure, we then studied the surface energy and chemistry of fracture surfaces. To characterize a very thin layer (0.5–1 nm), we used water-in-air contact angle measurement and SSIMS,[14,15] whose information, as shown in Part I of this work, is relative to a layer of the above-mentioned thickness and easily correlated.[8]

The results of water-in-air contact angle measurements are displayed in Table II. The advancing angle of water on the neat epoxy resin is slightly lower than that of untreated PP, whereas the receding angle is very low (high hysteresis), suggesting that its surface is more wettable than PP and also quite more heterogeneous. In the case of untreated PP–epoxy joints, the contact angles on the two sides are remarkably close to those of untreated PP and neat epoxy resin, respectively. Therefore, the fracture is clearly adhesive.

For plasma-treated samples, contact angles are those of untreated PP on both sides, suggesting that the fracture is cohesive (within untreated PP) and that the modified layer stays with the adhesive side. No effect of different curing cycles and preliminary thermal equilibration of oxygen plasma-treated PP was observed.

Table II Water Advancing (aa) and Receding (ra) Contact Angles (°) for PP/Epoxy Fracture Surfaces

Sample	Side	aa	ra
Untreated PP		95	80
E11 adhesive, cured 1 h at 353 K		90	18
E11 adhesive, cured 1 h at 353 K, untreated PP	1	95	80
	2	91	20
E11 adhesive, cured 1 h at 353 K, PP immediately after treatment	1	95	78
	2	95	79
E11 adhesive, cured 1 h at 353 K, PP aged 2 h 363 K	1	95	77
	2	95	77
E11 adhesive, cured 1 h at 393 K, PP immediately after treatment	1	95	77
	2	95	80
E11 adhesive, cured 1 h at 393 K, PP aged 2 h 393 K	1	95	81
	2	95	80

Sides 1 and 2 are not distinguishable on the basis of contact angle measurement, but XPS (see Table III) and FTIR-ATR allow unambiguous assignment of side 1 to the PP part and side 2 to the epoxy part.

The behavior observed by water-in-air contact angle measurement was further substantiated by SSIMS. As suggested in Part I, the use of $^{18}O_2$ plasmas is particularly useful, since the presence or absence of the peaks at 18 and 19 amu ($^{18}O^-$ and $^{18}OH^-$, respectively) states unambiguously whether oxygen introduced by the plasma treatment is present at the surface. Just-treated and thermally equilibrated (at 393 K) $^{18}O_2$ plasma-treated PP specimens were bonded using E11 adhesive and fractured by the usual procedure. Negative-ion SSIMS spectra relative to the two sides of the just-treated PP/epoxy joint are presented in Figure 1. They look identical, there is no trace of ^{18}O, and the amount of ^{16}O is well within that normally found on untreated PP samples (see Part I of this work, fig. 4-a). In the case of the thermally equilibrated sample, SSIMS spectra were very similar to those in Figure 1. The occurrence of the fracture within PP is then fully confirmed by SSIMS.

Fracture Surfaces: XPS

In XPS, the thickness of the observed layer depends in this case on the photoelectron escape depth. According to the electron mean free paths reported for polymers in conditions similar to ours,[16,17] a layer about 5 nm thick is observed.

XPS data relative to fracture surfaces of oxygen plasma treated PP/epoxy joints are presented in Table III. Side 1 has the typical composition of plain PP: It is the "PP" side. On side 2, oxygen and some silicon are present, but in lower amounts than in plasma-treated samples or plain E11 adhesive.[8] It is the "epoxy" side. Further confirmation of this evidence comes from the line-fitted C_{1s} photoelectron peaks in Figure 2. In Figure 2(a), the PP side is shown, which clearly looks like the untreated PP peak (see Part I, fig. 3-a). On the epoxy side [Figure 2(b)], some components relative to oxygen-containing functions are observed, in an amount lower than in plasma-treated samples (see Part I, figs. 3-b and 3-c).

This evidence indicates that on side 1 there is plain PP. On side 2, there is a multilayer structure, made of a thin layer of PP, then modified PP, and, finally, the E11 adhesive. The locus of failure is then within bulk PP but close to the modified layer. It is interesting to observe that the behavior is the same irrespective of thermal equilibration of plasma-treated PP samples and of the hardening cycle of the adhesive, confirming shear strength, contact angle, and SSIMS evidence (Tables I and II).

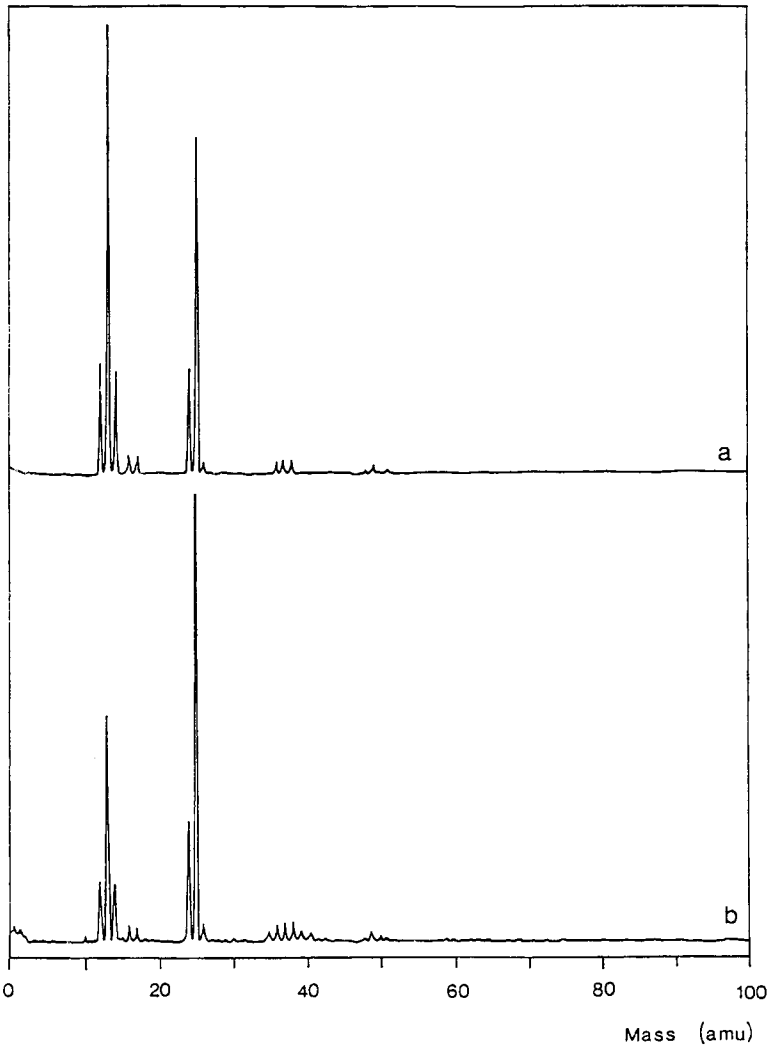

Figure 1 Negative ion SSIMS spectra relative to fracture surfaces of $^{18}O_2$ plasma treated PP/epoxy joints: side 1 (a), side 2 (b).

Fracture Surfaces: FTIR-ATR

FTIR-ATR allows us to observe a thicker layer, but the actual thickness depends on wavelength.[18] When using a germanium IRE and a 45° incidence angle, the thickness of the observed layer is about 0.3 μm at 3500 cm^{-1} and about 0.8 μm at 600 cm^{-1}.

In Figure 3, FTIR-ATR spectra relative to the two sides of an oxygen plasma-treated PP/epoxy fracture surface are shown. It is clear that on side 1 there is PP. On side 2, there is some PP, too, but bands relative to the epoxy adhesive are very intense, therefore confirming that the fracture site is close to the modified layer and to the epoxy adhesive.

Air-in-Water Contact Angles

Fracture surfaces relative to epoxy/oxygen plasma-treated PP (with or without thermal equilibration) joints were aged in water. The results are presented in Table IV. The main observation is that aging in water does not attract to the surface the polar groups introduced by the treatment, since the thin layer of bulk PP above the modified layer prevents the orientation at the surface of oxygen-containing groups observed in Part I of the work (Table IV). It is also interesting to note that the PP surfaces produced by fracturing an adhesive joint are actually more resistant to swelling by water than by molded PP surfaces, probably because of morphology and/or molecular weight effects.

Calculation of Fracture Energies

The above experimental results clearly suggest that the fracture occurs at the interface in the case of untreated PP/epoxy joints, whereas it occurs in the

Table III XPS Surface Composition of PP/Epoxy Fracture Surfaces

Sample	Side	C	O	Si
Untreated PP		98.2	1.8	
E11 adhesive, cured 1 h at 353 K		77.4	13.9	8.7
E11 adhesive, cured 1 h at 353 K, PP immediately after treatment	1	99.3	0.7	
	2	92.7	5.9	1.4
E11 adhesive, cured 1 h at 353 K, PP aged 2 h 363 K	1	97.2	2.1	0.7
	2	89.0	8.0	3.0
E11 adhesive, cured 1 h at 393 K, PP immediately after treatment	1	96.9	2.1	1.0
	2	92.3	5.2	2.5
E11 adhesive, cured 1 h at 393 K, PP aged 2 h 393 K	1	99.5	0.5	
	2	92.5	5.6	1.9

bulk of polypropylene, close to the interface, after oxygen plasma treatment of PP.

These results can be subjected to a surface energy analysis. In particular, as reviewed in Ref. 1, the fracture energy (consisting of reversible work of adhesion and irreversible plastic work contributions) and the work of adhesion itself can be calculated. Assuming the negligibility of mechanical interlocking and direct chemical bonding, the above-mentioned magnitudes have been related to polar and dispersion components of surface tension[12,13] or to the acid-base characteristics of polymers.[4,19]

The availability of contact angle data prompted us to calculate fracture energies using the method suggested by Kaelble[12] and reviewed by Wu.[1] Calculating work of adhesion, as suggested by Kinloch,[13] identical trends were observed.

In Table V, the relevant equations are presented. Equation (1) is the Griffith equation, describing the critical stress required to propagate a fracture.[1,12] The fracture energy (Γ_g) is the energy required to create one unit of interfacial area of crack; its calculation allows one to predict bond stability in a given environment.[1] Kaelble suggested obtaining fracture energies starting from contact angle data, via the calculation of the polar and dispersion components of the surface tension of the adhesive, the environment, and the adherend [eqs. (2)–(6)].[12,20]

To calculate the surface tension components, we measured contact angles of water and methylene iodide, as suggested by Wu[1] and Dalal.[21] Equilibrium contact angles should be used, but, as shown in Part I and Table II, large contact angle hysteresis was observed on plasma-treated PP and E11. In agreement with the work of Lamb and Furlong,[22] we chose to follow the recommendation of Wolfram and Faust,[23] who provided experimental and theoretical justification for the use as equilibrium angle the average of advancing and receding angles for systems with large hysteresis, but without surface roughness.

Table VI reports water and methylene iodide advancing and receding angles for untreated PP, E11 adhesive, and treated PP (after thermal equilibration, 2 h at 293 K). Immediately after plasma treatment, the surface tension of the treated PP surface is very high; therefore, meaningful methylene iodide contact angles cannot be obtained because of the spreading of the drop on the surface. The calculation of polar and dispersive components of surface ten-

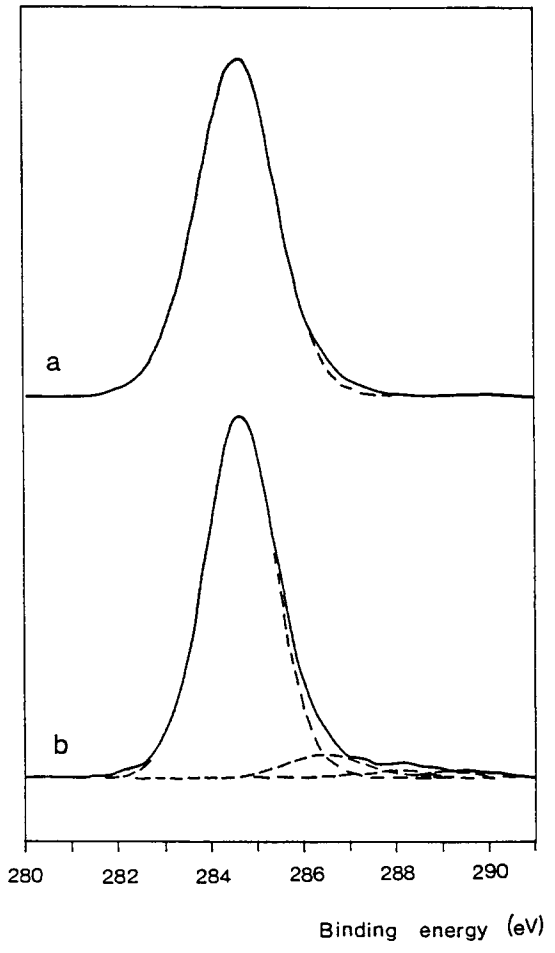

Figure 2 Line-fitted XPS C_{1s} peaks relative to the treated PP–epoxy fracture surfaces: (a) PP side, (b) adhesive side.

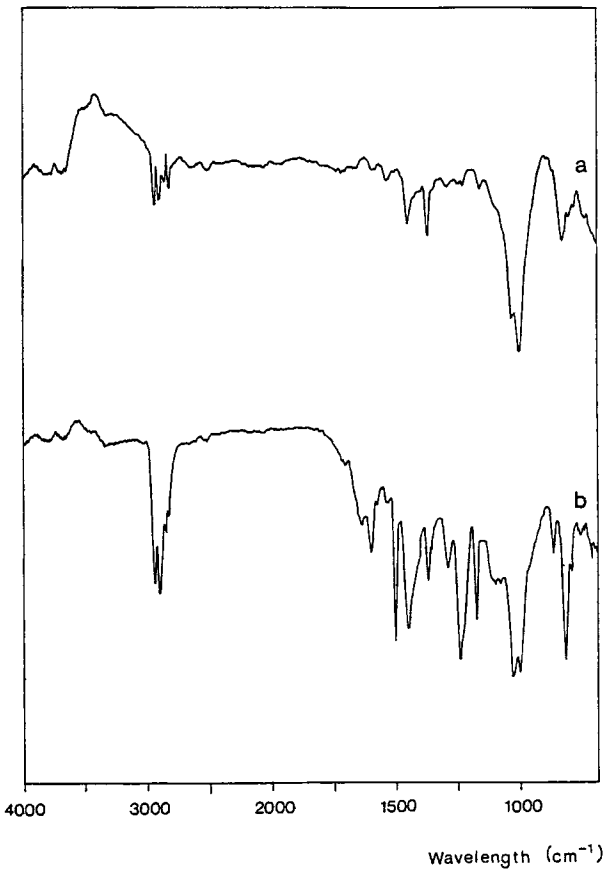

Figure 3 FTIR-ATR spectra of fracture surfaces relative to a just-treated PP/epoxy joint: side 1 (a), side 2 (b).

sion was performed using the geometric mean method[2,21]; the results are collected in Table VII.

By taking as equal to zero the surface tension components of the environment (air atmosphere), it is possible to calculate the fracture energies of all the possible loci of failure of our system, i.e., PP–PP, PP-treated PP, treated PP-treated PP, treated PP–E11, and E11–E11. Data are summarized in Table VIII and show that all the calculated values of fracture energy are positive, that is, all interfaces require a mechanical stress for debonding. If mechanical stress is applied, the cohesive fracture in PP is the most likely locus of failure, in agreement with experimental findings. These calculations have been performed in the case of thermally equilibrated PP, because of the impossibility of obtaining methylene iodide contact angles for just-treated PP. However, if high polar and dispersive components of surface tension (expected for just-treated PP) are introduced in eqs. (2)–(6), a very high fracture energy is obtained for the treated PP-epoxy interface, suggesting that also in this case the fracture is most probable in bulk PP.

DISCUSSION

The two kinds of adhesive joints we studied (untreated PP/epoxy and treated PP/epoxy) are quite different. Between untreated PP and epoxy adhesive, there is a single interface (PP/epoxy). The treated PP/epoxy system is three-layered: Bulk PP, modified PP, and epoxy layers are present. The modified layer is formed on top of bulk PP as a consequence of plasma treatment (see Part I); it can be described as a random copolymer containing oxidized and nonmodified PP units and is immiscible with bulk PP. The two interfaces are between modified PP and adhesive (sharp) and between modified PP and bulk PP (more diffuse).

The combination of techniques observing layers of different thickness of fracture surfaces (contact angle measurements and SSIMS: 0.5–1 nm; XPS:

Table IV Air-in-Water Advancing (aa) and Receding (ra) Contact Angles for Untreated and Oxygen Plasma-Treated PP as a Function of Aging Time in Water at 293 K

	Just-Treated PP				Thermally Equilibrated PP			
	Side 1		Side 2		Side 1		Side 2	
Time (h)	aa	ra	aa	ra	aa	ra	aa	ra
0	95	78	95	79	95	77	95	77
1	96	80	96	79	95	78	96	79
2	96	80	95	78	96	78	95	78
4	96	79	96	77	95	79	96	78
6	96	78	95	77	96	79	96	77
8	95	78	95	77	95	77	95	78
72	95	77	95	76	95	78	96	77
96	92	64	90	58	91	62	90	55

Table V Equations Relevant to the Obtainment of Fracture Energy Values According to Kaelble's Method[12,16]

$$\sigma_c = \left(\frac{2E\Gamma_g}{\pi C}\right)^{1/2} \quad (1)$$

$$\Gamma_g = R^2 - R_0^2 \quad (2)$$

$$R_0 = 0.25 \times [(\alpha_1 - \alpha_3)^2 + (\beta_1 - \beta_3)^2] \quad (3)$$

$$R = (\alpha_2 - H)^2 + (\beta_2 - K)^2 \quad (4)$$

$$H = 0.5\ (\alpha_1 + \alpha_3) \quad (5)$$

$$K = 0.5\ (\beta_1 + \beta_3) \quad (6)$$

Where σ_c = critical crack propagation stress; Γ_g = fracture energy; E = Young's modulus; C = crack length; α, β = square root of the dispersion and polar surface tension components of adhesive (1), environment (2), and adherend (3).

about 5 nm; FTIR-ATR 0.3–0.8 μm, depending on wavelength) allowed an interesting chemical depth profile and provided a completely unambiguous identification of the locus of failure of the above-mentioned joints.

In both untreated and plasma-treated PP samples, one side of the fracture surface is plain PP (side 1). In the untreated PP case, the other side (side 2) is the E11 adhesive. When plasma-treated specimens were used, three different layers are subsequently observed on side 2. The first is plain PP, with SSIMS (Fig. 1) and contact angles analyzed only this layer. The second is plasma modified PP; XPS (Fig. 2) allowed us to observe some oxygen relative to this layer, along with some silicon probably diffused from the adhesive in the form of siloxanes. Finally, the epoxy component was observed in FTIR-ATR spectra (Fig. 3). SEM showed that the morphology of fracture surfaces is smooth.

Experimental observations point in the case of plasma-treated PP, with or without thermal equilibration, to failure within bulk PP, but close to the bulk PP/modified PP interface. Fracture energy calculations suggest that in this case the locus of failure should be within bulk PP. The experimental evidence is then supported by surface energy analysis.

Now let us consider the strength of the adhesive joints. The result of contacting a plasma-treated PP with an epoxy resin is a stronger bond than in the case of untreated PP. But there is no significant difference between shear strengths relative to just-treated PP, and thermally equilibrated PP samples and also variations in the hardening cycle of the adhesive are ineffective in altering shear strength.

The weakness of the untreated PP/adhesive bond is clearly related to the lack of both polar and chemical interactions. In the case of treated PP, the strengthening of the bond is related to the change in chemistry of the PP surface layer. In fact, the smoothness of plasma-treated PP surfaces and fracture surfaces exclude mechanical interlocking as important for adhesion. The fact that for both just-treated and thermally equilibrated samples the same shear strength was observed is also interesting. Naively, a decrease might be expected in the case of the equilibrated sample because of the lesser amount of polar groups at the surface. However, our previous work on adhesion properties on surface-treated polypropylenes[24] showed that even a small number

Table VI Advancing (aa), Receding (ra), and Equilibrium (ea) Water and Methylene Iodide Contact Angles (°) for PP, Treated and Equilibrated PP, and E11 Surfaces

Substrate	Liquid	aa	ra	ea
Untreated PP	H_2O	95	80	87.5
	CH_2I_2	64	54	59
E11 adhesive	H_2O	90	18	54
	CH_2I_2	46	32	39
Treated and equilibrated PP	H_2O	95	50	72.5
	CH_2I_2	56	38	47

Table VII Dispersive and Polar Components of Surface Tension (mJ/m^2) for PP, Treated and Equlibrated PP, and E11 Surfaces, as Calculated by the Geometric Mean Method

Substrate	Dispersive Component	Polar Component
Untreated PP	26.7	3.6
E11 adhesive	32.6	19.0
Treated and equilibrated PP	31.3	8.6

Table VIII Fracture Energies (mJ/m^2) Assuming Different Loci of Failure

Locus of Failure	Fracture Energy
PP–PP	30.3
PP–treated PP	34.5
Treated PP–treated PP	39.9
Treated PP–E11	44.6
E11–E11	51.6

of polar groups is often enough to promote adhesion. Maybe chemical interactions between the modified layer and the epoxy resin occur, promoting the increase of shear strength.

In plasma-treated PP/epoxy joints, even if the fracture occurs within PP, the shear strength we observed is lower than might be expected for bulk PP.[25] This is in connection to the fact that the locus of failure is close to the modified PP/bulk PP interface. A possible interpretation is that different limiting factors act in untreated PP/epoxy and plasma-treated PP/epoxy joint strength. In the former case, the near-absence of polar and chemical interaction between PP and the adhesive is most important. In the case of plasma-treated samples, the dominant factor is not the chemical interaction but the mechanical strength of the PP surface layer, the so-called weak boundary layer.[1,5-7] That would also explain the overall indifference of both shear strength and locus of failure to both the thermal history of plasma-treated PP and the curing cycle of the adhesive. It is remarkable to note that, in the case of polyethylene, crosslinking and consequent strengthening of the weak boundary layer was observed after plasma treatment.[26] The difference lies probably in the fact that polypropylene is well known to be much less prone than polyethylene to crosslinking by interaction with energetic particles.[27]

CONCLUSION

The locus of failure of PP/epoxy joint is shifted by oxygen plasma treatment of PP. In the case of untreated PP, the fracture is adhesive because of lack of polar and/or chemical interaction between PP and the adhesive. In plasma-treated PP, it is cohesive within bulk PP, in agreement with fracture energy calculations, the dominating factor being probably the mechanical strength of the weak boundary layer.

We wish to thank Mrs. M. F. Gagliano, Dr. R. Marola, Mr. G. B. Morelli, Mr. L. Pozzi, and Mr. S. Soattini for experimental assistance.

REFERENCES

1. S. Wu, *Polymer Interface and Adhesion,* Marcel Dekker, New York, 1982.
2. M. Hudis, in *Techniques and Applications of Plasma Chemistry*, J. R. Hollahan and A. T. Bell, Eds., Wiley, New York, 1974, p. 113.
3. H. V. Boenig, *Plasma Science and Technology*, Cornell University Press, Ithaca, 1982.
4. F. M. Fowkes, *J. Adhes. Sci. Tech.*, **1**, 7 (1987).
5. K. L. Mittal, Ed., *Physicochemical Aspects of Polymer Surfaces*, Plenum Press, New York, 1983.
6. K. W. Allen, in *Proceedings of the 10th Annual Meeting of the Adhesion Society*, Williamsburg, VA, February 22–27, 1987.
7. L. H. Lee, Ed., *Recent Advances in Adhesion*, Gordon & Breach, New York, 1973.
8. E. Occhiello, M. Morra, G. Morini, F. Garbassi, and P. Humphrey, *J. Appl. Polym. Sci.*, to appear.
9. L. H. Lee, Ed., *Characterization of Metal and Polymer Surfaces*, Academic Press, New York, 1977.
10. M. Kerker, Ed., *Colloid and Interface Science*, Academic Press, New York, 1976.
11. L. Canova, F. Garbassi, and E. Occhiello, *J. Adhes. Sci. Tech.*, **1**, 319 (1987).
12. D. H. Kaelble, *Polym. Eng. Sci.*, **17**, 474 (1977).
13. A. J. Kinloch, in *Polymer Surfaces and Interfaces*, W. J. Feast and H. S. Munro, Eds., Wiley, New York, 1987.
14. W. A. Zisman, *Adv. Chem. Ser.*, **43**, 1 (1964).
15. M. J. Hearn, D. Briggs, S. C. Yoon, and B. D. Ratner, *Surf. Interface Anal.*, **10**, 384 (1987).
16. D. T. Clark, W. J. Feast, W. K. R. Musgrave, and I. Ritchie, *J. Polym. Sci. Chem. Ed.*, **13**, 857 (1975).
17. D. T. Clark and H. R. Thomas, *J. Polym. Sci. Chem. Ed.*, **15**, 2843 (1975).
18. F. M. Mirabella, *Appl. Spectrosc. Rev.*, **21**, 45 (1985).
19. F. M. Fowkes, in *Proceedings of the 10th Annual Meeting of the Adhesion Society,* Williamsburg, VA, February 22–27, 1987.
20. D. H. Kaelble and J. Moacanin, *Polymer*, **18**, 476 (1977).
21. E. N. Dalal, *Langmuir*, **3**, 1009 (1987).
22. R. N. Lamb and D. N. Furlong, *J. Chem. Soc. Faraday Trans. I*, **78**, 61 (1982).
23. E. Wolfram and R. Faust, in *Wetting Spreading and Adhesion*, J. F. Padday, Ed., Academic Press, London, 1978, Chap. 10.
24. F. Garbassi, E. Occhiello, and F. Polato, *J. Mater. Sci.*, **22**, 207 (1987).
25. R. B. Lieberman and P. C. Barbé, in *Encyclopaedia of Polymer Science and Technology,* Wiley, 1988, Vol. 13, p. 464.
26. H. Schonhorn, in *Polymer Surfaces*, D. T. Clark and W. J. Feast, Eds., Wiley, New York, 1978, p. 225.
27. V. D. McGinniss, in *Encyclopaedia of Polymer Science and Technology,* Wiley, 1986, Vol. 4, p. 418.

Received July 12, 1990
Accepted July 25, 1990